Recent results from T2K

S. Coleman

University of Colorado, Boulder
Boulder, CO 80309

Summary. — The T2K long baseline neutrino experiment uses a muon neutrino beam to measure the θ_{13} and θ_{23} neutrino oscillation mixing angles, as well as the neutrino mass state splitting Δm^2_{32}. The J-PARC facility has delivered 3.01×10^{20} protons to the T2K beamline as of July 2012. The experiment has observed muon neutrino disappearance and electron neutrino appearance consistent with neutrino oscillations. With ν_e appearance, T2K measures $\sin^2(2\theta_{13}) = 0.088^{+0.049}_{-0.039}$ ($0.108^{+0.059}_{-0.046}$) for $\delta_{CP} = 0$ and the normal (inverted) hierarchy. With ν_μ disappearance, the T2K preliminary measurement finds $\Delta m^2_{32} = 2.45 \times 10^{-3}\,\mathrm{eV}^2/\mathrm{c}^4$ and θ_{23} consistent with maximal mixing at 90% C.L.. These θ_{13} results are consistent with recent reactor experiments, and the θ_{23} is consistent with other accelerator-based disappearance experiments. T2K is currently taking data, and will improve these limits in the future.

PACS 14.60.Pq – Neutrino mass and mixing.
PACS 13.15.+g – Neutrino interactions.

1. – Introduction

The observation of neutrino flavor change is well established [1], and the energy-dependence of the observed disappearance is consistent with neutrino oscillations [2, 3]. Neutrino oscillations are described by a unitary matrix that relates neutrino mass states to neutrino flavor states:

$$\begin{pmatrix} \nu_e \\ \nu_\mu \\ \nu_\tau \end{pmatrix} = U_{\mathrm{PMNS}} \begin{pmatrix} \nu_1 \\ \nu_2 \\ \nu_3 \end{pmatrix} \tag{1}$$

where $U_{\rm PMNS}$ is the PMNS matrix, conveniently factorized as:

$$U_{\rm PMNS} = \begin{pmatrix} 1 & 0 & 0 \\ 0 & c_{23} & s_{23} \\ 0 & -s_{23} & c_{23} \end{pmatrix} \begin{pmatrix} c_{13} & 0 & s_{13}e^{-i\delta_{CP}} \\ 0 & 1 & 0 \\ -s_{13}e^{-i\delta_{CP}} & 0 & c_{13} \end{pmatrix} \begin{pmatrix} c_{12} & s_{12} & 0 \\ -s_{12} & c_{12} & 0 \\ 0 & 0 & 1 \end{pmatrix} \tag{2}$$

where $s_{ij} = \sin^2(\theta_{ij})$, $c_{ij} = \cos^2(\theta_{ij})$, and δ_{CP} is the CP-violating phase. While a neutrino is in flight (on terrestrial length scales), the quantum mechanical mass states interfere, gaining relative phase differences introduced by differences in their masses. This interference is observed experimentally in the fraction of neutrinos of one flavor oscillating into another. For muon neutrino beams, the probability that a ν_μ remains a ν_μ is

$$P_{\nu_\mu \to \nu_\mu} \approx 1 - \sin^2(2\theta_{23}) \sin^2 \left(1.27 \Delta m^2_{32} \frac{L(\text{km})}{E(\text{GeV})} \right) \tag{3}$$

where $\Delta m^2_{32} = m^2_3 - m^2_2$, the difference of the squares of the masses of two of the mass states, L is the distance the neutrino has traveled, and E is its energy. At this point in time, the sign of Δm^2_{32} is not known. This is called the mass hierarchy, and can be either normal ($m_3 > m_2$) or inverted ($m_2 > m_3$). The disappearance probability is related to the survival probability, $P_{\nu_\mu \to \nu_x} = 1 - P_{\nu_\mu \to \nu_\mu}$.

Observing ν_μ disappearance gives access to θ_{23} and Δm^2_{32} [4, 5]. The ν_μ oscillates primarily to ν_τ, and the appearance of ν_τ in a muon neutrino beam has also been established [6].

There is also a sub-dominant ν_e-appearance mode in a ν_μ beam:

$$P_{\nu_\mu \to \nu_e} \approx \sin^2(\theta_{23}) \sin^2(2\theta_{13}) \sin^2 \left(1.27 \Delta m^2_{32} \frac{L(\text{km})}{E(\text{GeV})} \right) + \text{sub} - \text{leadingterms} \tag{4}$$

where subleading terms include matter effects, solar terms, and CP violating and conserving terms. Electron neutrino appearance is dominated by the mixing angle θ_{13}, the last of the mixing angles to be determined. The appearance measurement is an important probe of the CP-violating phase δ_{CP} in $U_{\rm PMNS}$, which appears in higher-order terms in the ν_e-appearance probability. The value of δ_{CP} is at present unknown.

2. – The T2K experiment

The goal of the Tokai-to-Kamioka (T2K) experiment is to observe both sub-dominant electron neutrino appearance and muon neutrino disappearance in a muon neutrino beam. Thus T2K is able to measure both θ_{13} and θ_{23}.

The T2K experiment consists of a neutrino beamline, two major near detector systems, and a far detector. The muon neutrino beam used in T2K begins at the J-PARC facility, with a 30 GeV primary proton beam striking a graphite target. This interaction produces secondary pions and kaons that are focused by an electromagnetic focusing horn and then decay into tertiary neutrinos in a helium-filled decay pipe downstream of the target. The beam center is aimed 2.5° away from the far detector, using pion decay kinematics to produce a narrow-band off-axis beam. The beam flux is peaked in the energy region where muon neutrino disappearance probability is maximized. With a baseline of 295 km and $\Delta m^2 = 2.4 \times 10^{-3} \text{eV}^2/\text{c}^4$, this corresponds to neutrino energies around 0.6 GeV. The beam is pulsed every 2.5 s, allowing gating in the far detector, which reduces backgrounds from cosmic rays.

The off-axis angle is monitored with the on-axis Interactive Neutrino GRID (INGRID) detector, which consists of 16 steel-scintillator calorimeter modules arranged in the shape of a cross, located 280 m downstream of the graphite target. INGRID measures the rate of muon neutrino interactions in each module and

interpolates the beam profile. The beam direction is kept constant within 1 mrad, which corresponds to an energy shift of $< 2\%$ in the off-axis flux peak.

The off-axis beam flux is characterized by a near detector before any oscillations have occurred. The ND280 detector sits 2.5° off-axis, 280 m downstream of the graphite target. It is a heterogeneous detector, consisting of two Fine-Grained Detectors (FGDs), three Time-Projection Chambers (TPCs), an Electromagnetic Calorimeter (ECal), Side Muon-Range Detectors (SMRD), and a π^0 Detector (P0D). The P0D consists of alternating layers of detection planes and water bags. The detection planes are made up of scintillator bars, and the water bags have been emptied for future comparison of the neutrino cross-sections on carbon and water. The ND280 detector sits inside of the UA1 magnet, with a magnetic field strength of 0.2 T for muon momentum measurement and particle charge identification. The ND280 measurement constrains the ν_μ flux by detecting ν_μ and ν_e charged current (CC) events before any oscillations have occurred. It also constrains intrinsic beam ν_e and neutral current (NC) π^0 event rates.

The far detector is the Super Kamiokande (Super-K) water Cherenkov detector in the Kamioka mine, 295 km away from the graphite target. It is a tank of ultra-pure water with a fiducial volume of 22.5 ktons, instrumented with 11,000 PMT's. Muon neutrino and electron neutrino CC events are identified by the Cherenkov ring topologies observed from the outgoing lepton. Cosmic ray backgrounds are reduced by transmitting the GPS timing of each beam spill, and recording only PMT hits within 500 μs of the expected arrival time. Additional backgrounds originating outside of the fiducial volume are identified and rejected with the use of an optically isolated outer detector veto region.

2˙1. *Simulations.* – The beam flux simulations are tuned to proton beam monitors and the π and K fluxes measured from NA61 thin target data [7]. The π and K multiplicities are the dominant beam-related systematic errors. Neutrino interactions are simulated with the NEUT interaction model [8] in both the near and far detectors. Particle tracking and response in both the ND280 and Super-K detectors are simulated with GEANT3 [9].

2˙2. *Near-to-far Extrapolation.* – The near detector may be used to constrain systematic errors related to the neutrino beam and neutrino interaction cross-sections. Neutrino-induced CC ν_μ events in the ND280 tracker are separated by their momentum (p_μ) and their angle with respect to the beam (θ_μ), and whether or not the event has quasi-elastic (QE) topology.

The predictions of event rates in (p_μ, θ_μ) are parameterized with energy-dependent flux normalization parameters and a number of cross section parameters, including the ratio of ν_e to ν_μ cross sections, a scale factor for CC resonance production, and a scale factor for NC π^0 production. These parameters were chosen because they possess some correlation between the near and far detector event rates. Additional cross-section parameters without correlations between near and far are considered after the extrapolation proceedure. Prior values for the flux parameters come from beam monitor measurements and the NA61 uncertainties, as described in section **2˙1**. Prior values for the cross-section parameters come from MiniBooNE neutrino interaction data [10]. A fit is then performed with the observed ν_μ spectrum in ND280 and the parameterized predictions. The data and predictions are shown in fig. 1 before and after the fit. The addition of the ND280 constraint significantly reduces the magnitude of the systematic errors. The fit parameters and their covariance are then propagated to the far detector prediction. In the ν_e appearance analysis, this constraint reduces the combined size of the flux and cross-section systematic error on the predicted number of events by 40 to 60%, depending on the true value of $\sin^2(2\theta_{13})$ (see fig. 2).

3. – ν_e Appearance measurement

The appearance of ν_e in a ν_μ beam is measured by comparing the observed e-like single ring signal in the Super-K detector with all of the predicted backgrounds, including some irreducible beam ν_e contamination.

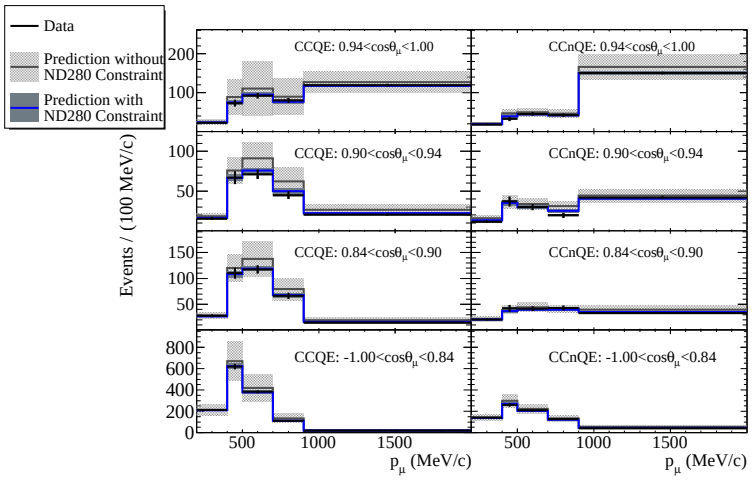

Fig. 1. – The ND280 ν_μ momentum (p_μ), and angle ($\cos\theta_\mu$) distribution and the Monte Carlo prediction before and after the fit to the ND280 ν_μ data. The error bars on the MC prediction represent the uncertainty from flux, cross section and detector systematic error sources. The highest momentum bins includes events with $p_\mu > 2000\,\mathrm{MeV/c}$, but is normalized by the bin width from 900-2000 MeV/c.

The other significant backgrounds for this measurement are non-QE or NC events that mimic the electron Cherenkov ring topology. Single high energy photons can convert to e^+e^- pairs and mimic an electron ring. One source of these photons are decays of $\pi^0 \to \gamma\gamma$, where one γ ring is lost (*i.e.* the two γ rings are overlapping, or one γ is absorbed). These π^0 are often the products of NC interactions, which carry no neutrino flavor information.

3˙1. *Selection.* – An electron neutrino CC interaction in Super-K is identified by an outgoing electron, which projects a Cherenkov ring on the wall of the detector. The electron Cherenkov ring topology is a ring with fuzzy edges due to e interactions within the water.

QE electron neutrino interactions are identified by requiring only one reconstructed ring that is electron-like, with no subsequent electron from μ-decay (Michel electron) that would indicate the presence of a muon. The total energy visible in the event must be $> 100\,\mathrm{MeV}$. Due to the narrow-band off-axis beam, the signal region is sharply peaked, and intrinsic beam ν_e and NC backgrounds are reduced by requiring the reconstructed energy of the neutrino event be $< 1250\,\mathrm{MeV}$. Finally, backgrounds from NC π^0 events are reduced by forcing the reconstruction to make its best guess of a second ring somewhere in the detector, and then requiring that the invariant mass of the particle in the 2-ring hypothesis is less than 105 MeV.

3˙2. *Systematic Uncertainties.* – Some systematic uncertainty remains after the extrapolation procedure described in sec. **2**˙2 is performed. Additional neutrino cross section uncertainties not correlated between the near and far detectors are left unconstrained. In addition, there are significant uncertainties related to the particles remaining in the final state, and secondary interactions with the water. A summary of systematic uncertainties is shown in tab. I, for two values possible of $\sin^2(2\theta_{13})$.

3˙3. *Results.* – Between January 2010 and June 2012, 3.01×10^{20} protons on target (POT) were delivered to T2K. This period of time includes recovery efforts from the March 2011 earthquake. This represents 4% of the beam exposure that is intended for T2K. With this exposure, the expected background is 3.22 ± 0.43 events (see breakdown in tab. II). In total, 11 ν_e candidate events were observed. The probability of the background fluctuating up to 11 events is 0.08%, corresponding to 3.2σ significance exclusion of the no-appearance hypothesis.

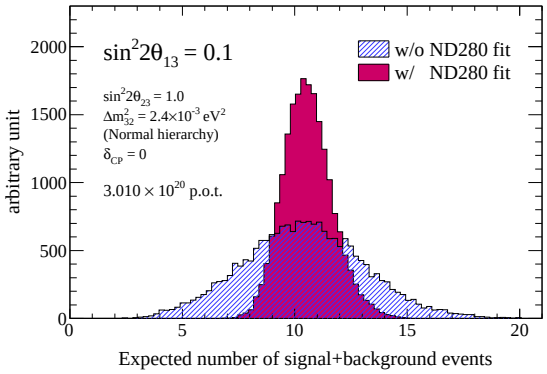

Fig. 2. – Distribution of systematically shifted predictions of $N_{\rm exp}$ at the Super-K detector before and after the inclusion of the ND280 constraint. All assumed parameter values are shown in the box above. The ND280 constraint reduces the overall size of the flux and cross-section systematic error on the expected number of events by 60%, assuming $\sin^2(2\theta_{13}) = 0.1$.

Event rate and kinematics information are included when the data is used to extract $\sin^2(2\theta_{13})$. A two-dimensional extended maximum likelihood fit is performed using the apparent momentum (p_e) and angle with respect to the beam (θ_e) of the outgoing lepton. Results are reported for all values of δ_{CP}, for both the normal and inverted mass hierarchies. Assuming $\delta_{CP} = 0$, $\sin^2(2\theta_{13}) = 0.088^{+0.049}_{-0.039}$ $(0.108^{+0.059}_{-0.046})$ for the normal (inverted) mass hierarchy [12]. The 68% and 90% C.L. allowed regions are shown in fig. 3.

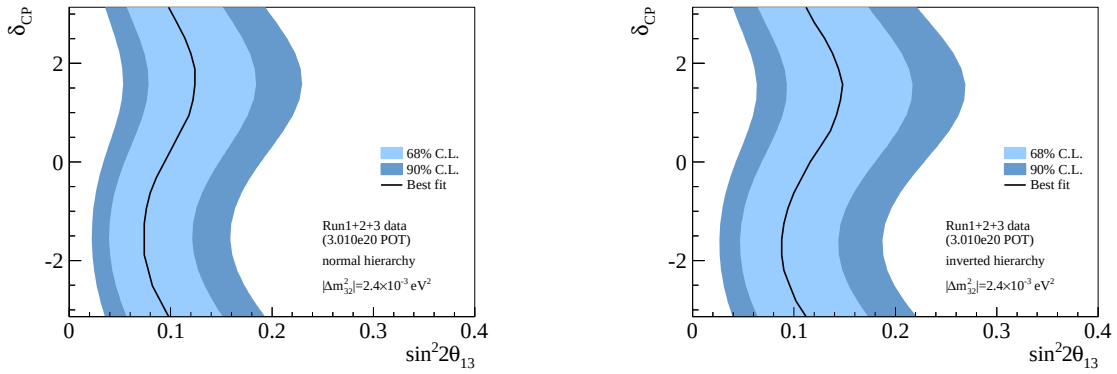

(a) (b)

Fig. 3. – The T2K allowed regions, assuming the normal mass hierarchy (fig. 3(a)) and inverted mass hierarchy (fig. 3(b)).

Error	$\sin^2(2\theta_{13}) = 0.0$	$\sin^2(2\theta_{13}) = 0.1$
Beam	8.5	5.0
ν interactions	5.9	7.4
Final state interactions	2.9	2.3
Far Detector	6.8	3.0
Total	13.0	9.9

Table I. – *Systematic uncertainties, in units of percent, for each systematic category in the ν_e appearance measurement.*

4. – ν_μ Disappearance measurement

The disappearance of ν_μ in a ν_μ beam is measured by comparing the predicted ν_μ spectrum without neutrino oscillations with that observed in the detector. With a larger number of events both predicted and observed, the shape of oscillated ν_μ spectrum provides more information than the shape of the spectrum in the ν_e appearance. With this preliminary measurement, two independent methods are used to determine the allowed region in the parameter space $\Delta m^2_{32} - \sin^2(2\theta_{23})$. One is a likelihood ratio method using the reconstructed neutrino energy spectrum (E_ν) in a fit that includes 48 nuisance parameters, representing all systematic uncertainties. The second method is a maximum likelihood method with reconstructed E_ν, which calculates the maximum likelihood as the product of the signal normalization likelihood, an unbinned shape likelihood, and a likelihood of systematic error parameters. Both methods construct allowed regions of parameter space following the Feldman-Cousins prescription [13].

4˙1. *Selection.* – A muon neutrino interaction in Super-K is identified by an outgoing muon, which is identified by a Cherenkov ring in water. Muons make Cherenkov rings with sharp edges, as they travel long distances without showering or scattering. Muon rings may also be filled in toward their centers as the muon approaches the Cherenkov threshold.

Quasi-elastic muon neutrino interactions are selected by requiring each event has only one reconstructed ring that is muon-like, and the reconstructed momentum of the muon must be $> 200\,\mathrm{MeV}$. Fewer than 2 Michel electrons are allowed to be reconstructed in the event. The selected signal still contains some non-QE muon neutrino interactions, and CC π production and NC single-π productions are the main backgrounds.

4˙2. *Systematic Uncertainties.* – The ν_μ disappearance analysis makes use of the same near detector constraint described in sect. **2˙2**. Additional systematics include cross section uncertainties that are not correlated between the near and far detectors, far detector selection efficiencies for CC and NC events, and uncertainties in the final state interaction in the nucleus and the secondary interaction of the particles in the water. The dominant systematics are shown in tab. III.

4˙3. *Preliminary Results.* – The disappearance analysis uses the same data set as described in sect. **3˙3**, with $3.01 \times 10^{20}\,\mathrm{POT}$. The observed ν_μ signal is shown in fig. 4, compared to the no-oscillation hypothesis. Both analysis methods found the signal to be consistent with maximal mixing, $\sin^2(2\theta_{13}) = 1.0$ and $\Delta m^2_{32} = 2.443 \times 10^{-3}\,\mathrm{eV}^2/\mathrm{c}^4$, for the likelihood ratio method, and $\Delta m^2_{32} = 2.45 \times 10^{-3}\,\mathrm{eV}^2/\mathrm{c}^4$ for the maximum likelihood method. The allowed regions for these two methods, compared to results from other experiments, are shown in fig. 5.

5. – Conclusion

The T2K experiment has accumulated only 4% of its target beam exposure, with 3.01×10^{20} protons-on-target. With this dataset, we observed the first appearance of ν_e in a ν_μ beam, and have made measurements

	$\sin^2(2\theta_{13}) = 0.0$	$\sin^2(2\theta_{13}) = 0.1$
CCν_e signal	0.2	8.2
CC Beam ν_e	1.8	1.7
CC ν_μ	0.06	0.06
NC	1.2	1.2
Total	3.3	11.2

TABLE II. – *The predicted number of events in each category, assuming no oscillations (*$\sin^2(2\theta_{13}) = 0$*) and oscillations consistent with reactor experiments like Daya Bay [11].*

of θ_{13} that are consistent with measurements of θ_{13} derived from reactor-sourced antineutrino disappearance [11, 15]. We have also made measurements of ν_μ disappearance that are consistent with MINOS and Super-K [4, 5]. Future T2K precision measurements of θ_{13} and θ_{23}, combined with other experiments, will put limits on the value of δ_{CP} and resolve the mass hierarchy.

REFERENCES

[1] Beringer, J. et al. Jul 2012 *Phys. Rev. D* **86**, 010001.
[2] Pontecorvo, B. (1958) *Sov. Phys. JETP* **7**, 172–173.
[3] Maki, Z., Nakagawa, M., and Sakata, S. (1962) *Prog. Theor. Phys.* **28**, 870–880.
[4] Adamson, P. et al. May 2011 *Phys. Rev. Lett.* **106**, 181801.
[5] Wendell, R. et al. May 2010 *Phys. Rev. D* **81**, 092004.
[6] Agafonova, N. et al. (2010) *Phys. Lett. B* **691(3)**, 138 – 145.
[7] Abgrall, N. et al. (2013) *Nucl. Instr. Meth. Phys. Res. A* **701(0)**, 99 – 114.
[8] Hayato, Y. (2009) *Acta Phys.Polon.* **B40**, 2477–2489.
[9] Brun, R. et al. Geant3 users guide Technical report CERN DD/EE/84-1 (1987).
[10] Aguilar-Arevalo, A. A. et al. May 2010 *Phys. Rev. D* **81**, 092005.
[11] An, F. P. et al. Apr 2012 *Phys. Rev. Lett.* **108**, 171803.
[12] Abe, K. et al. (2013).
[13] Feldman, G. J. and Cousins, R. D. Apr 1998 *Phys. Rev. D* **57**, 3873–3889.
[14] Abe, K. et al. Feb 2012 *Phys. Rev. D* **85**, 031103.
[15] Ahn, J. K. et al. May 2012 *Phys. Rev. Lett.* **108**, 191802.

Error	Syst. error
Flux and ν interaction	4.2
Other ν interactions	6.3
Super-K Detector	10.1
Final and secondary-state interactions	3.5
Total	13.0

TABLE III. – *The 1σ systematic error on the total number of observed ν_μ events, in units of percent, for the ν_μ disappearance measurement. These errors assume $\Delta m^2_{32} = 2.4 \times 10^{-3}\, eV^2/c^4$ and $\sin^2(2\theta_{23}) = 1.0$.*

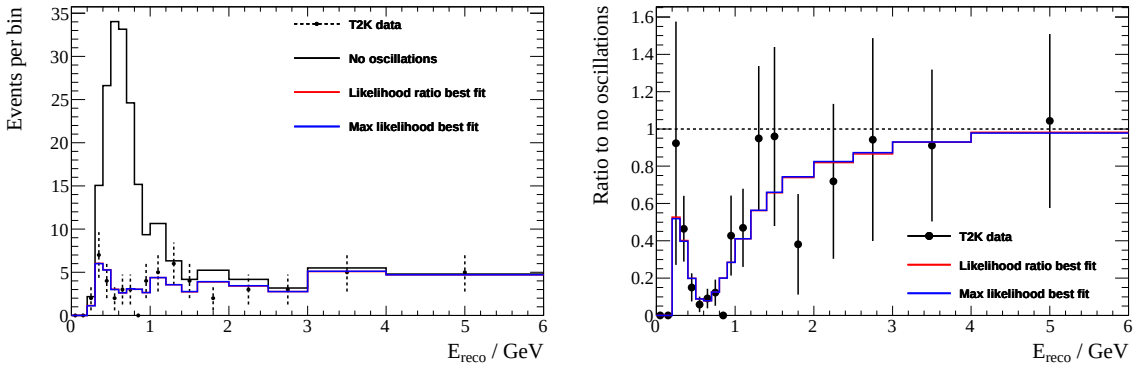

(a) (b)

Fig. 4. – On the left, the predicted muon neutrino energy spectrum without neutrino oscillations, compared with the data and the best fit to data with neutrino oscillations. On the right, the ratio of the data and the best fit to the no-oscillation hypothesis.

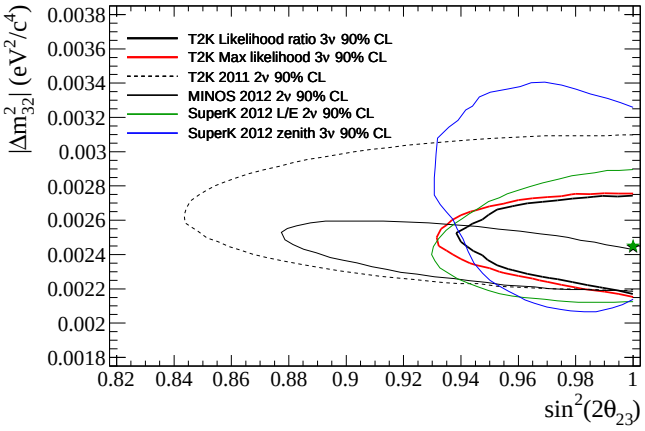

Fig. 5. – Preliminary allowed regions for the two T2K analysis methods described here, combined with the allowed region from an earlier result [14] and allowed regions from other experiments [4, 5].